Noise study of a high-T_c Josephson junction under near-millimeter-wave irradiation

R. Gupta and Qing Hu
Department of Electrical Engineering and Computer Science and Research Laboratory of Electronics, Massachusetts Institute of Technology, Cambridge, Massachusetts 02139

D. Terpstra, G. J. Gerritsma, and H. Rogalla
Department of Applied Physics/Low Temperature Division, University of Twente, 7500 AE Enschede, The Netherlands

Noise studies of both the dc and ac Josephson effects have been performed on a high-T_c ramp-type Josephson junction irradiated at 176 GHz. Well-established analytical results for noise in over-damped RSJs are used to model the measured I-V characteristics, and their agreement is excellent. Noise-rounded I-V curves at the critical current and the first and second Shapiro steps under coherent 176 GHz radiation have been studied in detail at several temperatures and rf power levels. The noise temperatures inferred from these simulations are close to the physical temperatures. An increase of noise temperatures at high radiation power levels is a result of radiation heating, which could be due to a bolometric effect.

The possibility of using high-T_c Josephson junctions as far-infrared detectors and mixers at operating temperatures above liquid nitrogen relies on a quantitative knowledge of how various noise sources affect junction current-voltage (I-V) characteristics. Noise can diminish the response of sensitive detectors by rounding some nonlinear characteristics used in direct detection and mixing, and in extreme cases, by washing out the features completely.

To date, two notable noise studies have been performed on the experimental I-V characteristics of high-T_c Josephson junctions.[1,2] In Ref. 1, Monte Carlo simulations were used to model the noise effects on the reduction of amplitudes of the critical current and first two Shapiro steps in an rf-current-biased regime at microwave radiation frequencies (rf) below 10 GHz. In Ref. 2, the authors estimated the noise temperature T_N as a function of the physical temperature T_P by measuring the temperature dependence of the linewidth of millimeter-wave Josephson oscillations near the first Shapiro step at 70 GHz. The work presented here follows the studies on low-T_c devices, which used well-established theories developed for an overdamped resistively shunted-junction (RSJ) model, by directly modeling the I-V characteristics of the junction.[3–5] We undertake a more systematic study of noise measurements by investigating the junction in two domains: One in which the physical temperature is varied and its effect on the critical current and the radiation-induced steps are investigated, and the other in which rf power levels are varied and their contributing effects are studied.

The noise measurements described in this letter are performed on a previously studied junction.[6] The fabrication techniques, the quasioptical scheme, the temperature regulation stage, and the noise reduction system are thoroughly described in the reference. In the earlier work, we found the junction to exhibit highly RSJ-like characteristics and to be rf-voltage-biased under coherent radiation at 176 GHz. Such behavior, which illustrates the ideal characteristics found in low-T_c devices, is crucial to the investigation presented here.

Classically overdamped RSJs with zero capacitance in the presence of white noise were initially investigated by Ambegaokar and Halperin (A&H) for the noise-rounded characteristics of the critical current step.[7] Stephen showed their result was also valid for the rounding of the radiation-induced integer Shapiro steps in an rf-voltage-biased regime.[8] Lee extended this case to include the effects of finite capacitance and finite radiation linewidth.[9] Since our junction characteristics fall within the limits of Stephen and Lee, we have a unique opportunity to study the noise characteristics of a high-T_c junction based on their analysis. In addition, the analytical nature of their theoretical results allows simple and detailed comparison between experiment and theory.

Noise effects on junction behavior are exhibited by the rounding of the sharp corner transitions from the constant voltage states near the critical current and the Shapiro steps to the "running states" that exhibit finite differential resistance. This rounding results from a dephasing of the Josephson pair current due to thermal activation. The susceptibility to noise is greatest in these transition regions and this is where most of the fitting is done. Pure white noise, defined as having a δ-function time autocorrelation function, or equivalently, a uniform power spectrum, is representative of the thermal noise investigated here. Its effect on the junction characteristics is given in the following set of equations:

$$\delta V = \frac{\Delta I_n R_n}{2\gamma}\left(1 - e^{-2\pi\gamma\delta I_n/\Delta I_n}\right)\frac{1}{T_1}\left(1 + \beta_c\frac{T_2}{T_1}\right), \qquad (1)$$

where

$$T_1 = \int_0^\pi I_0(\gamma \sin \phi)e^{-2\gamma\phi\delta I_n/\Delta I_n}d\phi \qquad (2)$$

and

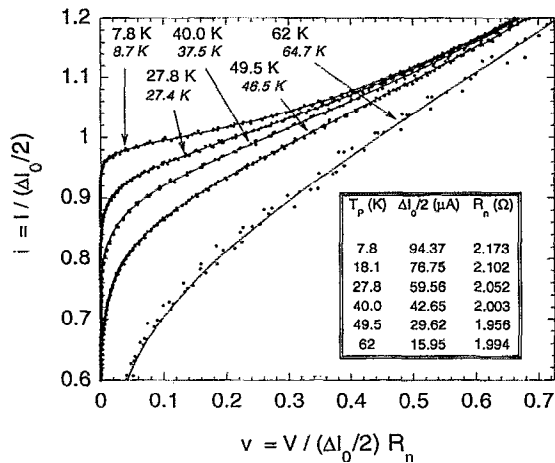$$T_2 = \int_0^\pi \sin \phi I_1(\gamma \sin \phi)e^{-2\gamma\phi\delta I_n/\Delta I_n}d\phi. \qquad (3)$$

FIG. 1. Sample experimental I-V curves (dots) at selected physical temperatures T_P are taken of the critical current near its region of high nonlinearity and fitted with I-V curves calculated from Eqs. (1)–(3) (solid lines). The theoretical noise temperature T_N from the simulations are found in italics. The current and voltage scales are normalized and the scaling parameters used are found in the inset.

Here, δV is the actual voltage measured from the center of a given step number n, ΔI_n is the total amplitude of the noiseless current step, δI_n is the current measured from the center of the nth step for $\delta I_n \lesssim \Delta I_n/2$, and R_n is the voltage-independent normal-state resistance as found in the RSJ. The Stewart–McCumber parameter β_c is equal to $(e\Delta I_n C/\hbar)R_n^2$, and γ is equal to $\hbar \Delta I_n/2ek_B T_N$. Together they give a com-

plete description of the noise in the system. We employed a computer simulation program to produce fits to Eq. (1), allowing the three fitting parameters ΔI_n, R_n, and T_n to be extracted. The capacitance is estimated to be about 1.5 fF and β_c, which is proportional to ΔI_n, and is maximal at 3×10^{-3}.[6]

The plasma frequency ω_p, equals to $(e\Delta I_n/\hbar C)^{1/2}[1-(2\delta I_n/\Delta I_n)^2]^{1/4}$ defines the peak frequency of junction noise responsivity. The Lorentzian linewidth of this responsivity has a quality factor proportional to $\beta_c^{1/2}$, and is quite broad for the junction investigated here. Nevertheless, the ability to control the value of ΔI_n and δI_n, and therefore ω_p, either by changing the operating temperature or by applying radiation, enables us to investigate the noise effect on the junction behaviors over a broad frequency range.

Simulated curves were overlaid on the experimental data for visual inspection and an estimate of the fitting quality χ^2 was calculated by the simulation package using the Levenberg–Marquardt least-squares method.[10] χ^2 was on the order of 10^{-4} or better. However, the accuracy of predicted noise temperature is within 10% for any given curve because of errors in possible scaling offsets of the measurement apparatus and errors due to the discrete nature of the digital sampling used. Additionally, the effect of a finite radiation linewidth is neglected because of the narrow linewidth (<10 MHz) of our Gunn oscillator-pumped doubler.

The experimental data were taken to include the inflection point just beyond the step in order to add a certain rigidity to the fits by pinning the experimental data and its fit at this point. Modeling of the first and second current steps required guessing the location of the steps' centers. Thus, the fits were done on both the positive- and negative-going parts of the curve as it extends away from the step, assuming symmetry in both directions. In some case, it was necessary
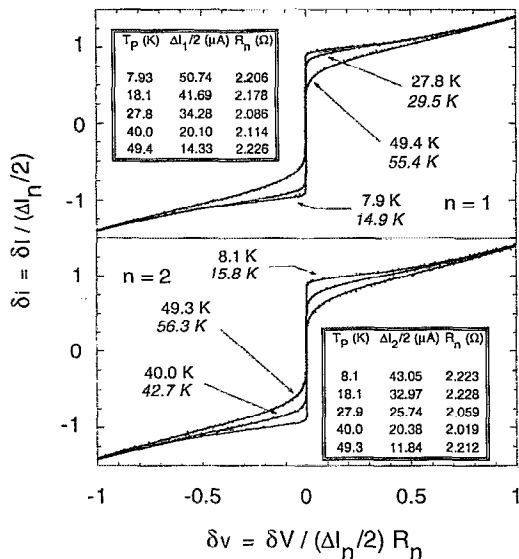

FIG. 2. Similar to Fig. 1, the first ($n=1$) and second ($n=2$) steps under 176 GHz radiation are plotted against theoretical noise-rounded I-V curves. Again, the physical temperatures are given next to the curves in plain text and the estimated noise temperatures in italics. Both positive- and negative-going ends of the steps show good symmetry. The axes are scaled by parameters found in the inset, and the curves are fit around the center of the step where δi and δv represent the current and voltage offsets, respectively, from the center.
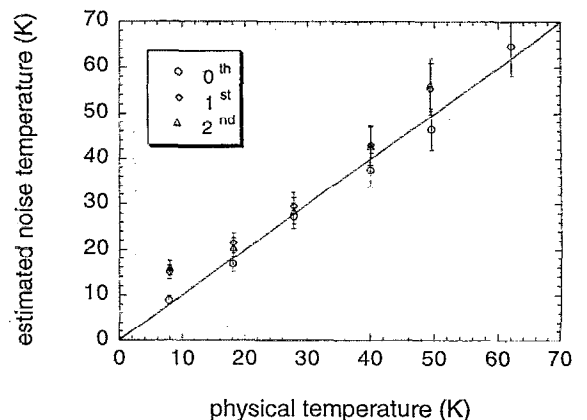

FIG. 3. The estimated noise temperatures at the critical current and the first and second steps are plotted vs the physical temperature. The error bars result from possible errors in the measurement apparatus and do not represent inconsistencies of fitting data. The first and second step amplitudes are biased to be maximal at 176 GHz; no radiation is incident for the measurement of the critical current. The dashed line of slope one gives the noise temperature to be equal to the physical temperature.

to do each half-separately due to a slight asymmetry. Nevertheless, the noise temperature estimations presented here are representative of all the results obtained.

Figures 1 and 2 indicate the coincidence of the simulated curves to the experimental data. The current and voltage scales are normalized using ΔI_n and R_n. δI_n and δV_n are the magnitude in current and voltage, respectively, from the center of nth step. The scales are greatly expanded to show the individual data points. For fitting, however, the data points extended in a range two to three times greater than that shown in either figure. In Fig. 2, the first and second steps are biased at radiation power levels such that each is individually maximal at any given temperature, which correspond to $2\alpha = 2eV_{rf}/\hbar\omega \approx 2$ and 3, respectively, where V_{rf} is the magnitude of the rf voltage induced across the junction.[6] This allows better resolution by our measurement apparatus and cleaner fits.

An estimate of the calculated noise temperatures versus the physical temperatures for a complete set of curves similar to those in Figs. 1 and 2 is presented in Fig. 3. Radiation levels are held constant for both the first and second step throughout the various temperatures. No radiation is applied during the measurement of the critical current step. Measurements were conducted on the junction up to temperatures where thermally induced flux transport becomes significant and affects the extended I-V characteristics of the step investigated. This limit was near 62 K for the critical current, but was only near 50 K for both the first and second step.

We see that noise in excess of that in the bath environment is not significant throughout the temperature range explored. The noise temperatures of the first and second steps are consistently above the physical temperatures, and possibly result from heating due to the radiation (a bolometric effect) or static bias dissipation.

Concentrating further on additional noise from the incident radiation, we focused on increasing the rf power levels at lower physical temperatures. This would allow better reso-

lution of the critical current and the first and second steps. These noise temperatures are plotted in Fig. 4 as a function of attenuation (in dB) of the maximal available rf power, where the physical temperature is between 8–9 K. We find a constant extra noise at small rf power levels whose origin is unknown. The static bias dissipation V^2/R_n, which is near 0.065 μW at the first step and four times that amount at the second step, is negligible. However, at our highest rf power level, we estimate that rf power dissipation $V_{rf}^2/2R_n$ is near 1 μW for $2\alpha \approx 5.5$ and $V_{rf} \approx 2$ mV.[6] At this absorbed radiation power level, the noise temperature is about 10 K higher than the physical temperature of the thermal stage, indicating that the local electronic temperature is raised by the radiation. Assume this is a microbolometric effect,[11] that is, the electrons are in thermal equilibrium with the local phonon system, the thermal conductance G between the Josephson junction and the thermal bath can then be estimated to be $G \approx 1$ μW/10 K $= 10^{-7}$ W/K. G can also be calculated using the formula for the thermal spreading conductance of a microbolometer, $G = (2\pi A)^{1/2}\kappa$, where A is the contact area between the junction and the substrate and κ is the thermal conductivity of the substrate material.[11] For our device, $A \approx 5$ μm^2, and $\kappa \approx 3 \times 10^{-3}$ W/cm K for YSZ at 10 K.[12] Thus, $G \approx 2 \times 10^{-6}$ W/K, which is about one order of magnitude larger than the value of G estimated from our measurement and simulation. The smaller inferred thermal conductance, or the additional thermal resistance, could result from a thermal boundary resistance R_{bd} between the YBCO film and the yttrium-stabilized cubic ZrO$_2$(YSZ) substrate.[13] For $A \approx 5$ μm^2 and $G \approx 10^{-7}$ W/K, $R_{bd} = A/G \approx 0.5$ K cm^2/W, which is about two orders of magnitude larger than the measured value at 100 K.[13] The origin of this surprisingly large thermal resistance between the junction and the bath will be a subject of further investigation.
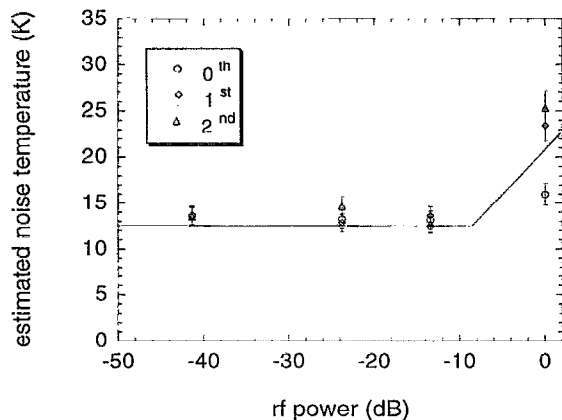
FIG. 4. Near 8 K, the noise temperatures are plotted as a function of the radiation power level at 176 GHz, given as dBs of attenuation of the maximal rf power. Note the significant increase in noise temperature at the maximal power level due to a bolometric effect. The dotted lines serve only as eye guides.

[1] R. L. Kautz, R. H. Ono, and C. D. Reintsema, Appl. Phys. Lett. **61**, 20 (1992).

[2] Y. Y. Divin, J. Mygind, N. F. Pedersen, and P. Chaudhari, Appl. Phys. Lett. **61**, 3053 (1992); Y. Y. Divin, A. V. Andreev, G. M. Fischer, J. Mygind, N. F. Pedersen, K. Herrmann, V. N. Glyantsev, M. Siegel, and A. I. Braginski, Appl. Phys. Lett. **62**, 1295 (1993).

[3] J. T. Anderson and A. M. Goldman, Phys. Rev. Lett. **23**, 128 (1969).

[4] M. Simmonds and W. H. Parker, Phys. Rev. Lett. **24**, 876 (1970).

[5] W. H. Henkels and W. W. Webb, Phys. Rev. Lett. **26**, 1164 (1971).

[6] R. Gupta, Q. Hu, D. Terpstra, G. J. Gerritsma, and H. Rogalla, Appl. Phys. Lett. **62**, 3351 (1993).

[7] V. Ambegaokar and B. I. Halperin, Phys. Rev. Lett. **22**, 1364 (1969).

[8] M. J. Stephen, Phys. Rev. **186**, 393 (1969).

[9] P. A. Lee, J. Appl. Phys. **42**, 325 (1971).

[10] W. H. Press, B. P. Flannery, S. A. Teukolsky, and W. T. Vetterling, *Numerical Recipes in C* (Cambridge University Press, Cambridge, England, 1988), Chap. 14.

[11] Qing Hu and P. L. Richards, Appl. Phys. Lett. **55**, 2444 (1989).

[12] D. A. Ackerman, D. Moy, R. C. Potter, A. C. Anderson, and W. N. Lawless, Phys. Rev. B **23**, 3886 (1981).

[13] M. Nahum, S. Verghese, and P. L. Richards, Appl. Phys. Lett. **59**, 2034 (1991).